Ultraslow strain rate measurement system for ice using phase modulation homodyne interferometer

Masato Aketagawa[1#], Nobuhiko Azuma[1], Morimasa Takata[1], Ryota Sugawara[1], Reo Ito[1], Kazuki Anno[1], Takahiro Kogure[1] and Yasuharu Ohba[1]

1 Department of Mechanical Engineering, Nagaoka University of Technology, Kamitomioka, Nagaoka, Japan, 940-2188
Corresponding Author / E-mail: masatoaa@vos.nagaokaut.ac.jp, TEL: +81-258-47-9741, FAX: +81-258-47-9770

KEYWORDS: Interferometer, Phase modulation, Ice deformation, Strain rate

The analysis of the flow behavior of the Antarctic ice sheet provides information on past climate changes of Earth. To understand the ice sheet flow behavior, the ice creep strain rate measurements with various stresses are important. In this study, an ice creep strain rate measurement system with an uncertainty of order less than $10^{-10}s^{-1}$ and a minimum measurement time of 10minutes is developed. The ice specimen of interest is set in a low-constant-temperature room and cell, with a set-point temperature and a maximum stability of -30~-10˚C and +-20mK or less, respectively. A modified phase modulation homodyne interferometer, the supporting material of which is ultralow-thermal-expansion glass, is combined with the system to measure the ice deformation with the resolution of nanometer scale or less. In this paper, the operational principle, instrumentation and experimental results are discussed.

Manuscript received: January XX, 2011 / Accepted: January XX, 2011

1. Introduction

Antarctica and Greenland are covered with ice sheets. The snow accumulates on the ice sheets along with a variety of dust and particles, and therefore, information on the paleo-environment and climate of the earth are preserved within the frozen stratigraphic layers of ice sheets. The analysis of the flow behavior of the Antarctic ice sheet provides information on past climate changes of Earth. To understand the ice sheet flow behavior, the ice creep strain rate measurements with various stresses are important. The Antarctic ice sheet flows at the strain rate of 10^{-13} to $10^{-10}s^{-1}$ with stress below 0.1MPa. In the conventional strain measurement, the dial gauge or transducer with the resolution of 0.1mm order is used. Therefore, it takes several hundred of hours to obtain a detectable displacement for a deformation of a specimen 10 cm long with the strain rate of $10^{-11}s^{-1}$.

In this study, an ice creep strain rate measurement system with an uncertainty of $10^{-10}s^{-1}$ or less and a minimum measurement time of 10minutes is developed. The ice specimen of interest is set in a low-constant-temperature room and cell, with a set-point temperature and maximum stability of -30~-10 ˚C and +-20mK or less, respectively. A modified phase modulation homodyne interferometer [1, 2], the supporting material of which is ultraslow-thermal-expansion glass (ULTEG), is combined with the system to measure the ice deformation with the resolution of nanometer or less. In this paper, the operational principle, instrumentation and experimental results are discussed.

2. Instrumentation

2.1 Whole System

Fig. 1 shows the whole system used for ice strain measurement. The system has three rooms A, B and C. The inside of room A is kept at a temperature of 20+-1˚C for the He-Ne lasers and precision measurement instruments, room B is kept at a temperature of -30 - -10˚C with a stability of 20mK or less for the ice specimen and an interferometer, and in room C, the heat from room B is dispersed to outside. In room A, an iodine-frequency-stabilized He-Ne laser, its frequency offset He-Ne laser and optics (a Faraday rotator: FR, a half-wave plate 1: HWP1, an electric optic modulator: EOM and a polarization-maintaining-single-mode-fiber: PM fiber) are installed on a passive antivibration table. A personal computer (PC) with a digital signal processor (DSP) and interfaces, lock-in amplifiers (LIAs), an oscillator (OSC) and displays with

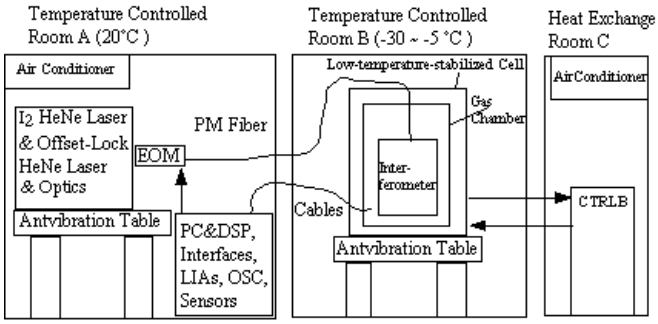

Fig. 1 Ice strain rate measurement system. EOM: Electric optical modulator, PM fiber: Polarization maintaining single mode fiber, Interfaces: Analogue-to-digital converter (ADC) + Digital-to-analogue converters (DAC) + RS232C, Sensors: Pressure and temperature sensors, CTRLB: constant temperature refrigerant liquid bath, LIAs: Lock-in amplifiers, OSC: Oscillator.

electronics for sensors (temperature and pressure) are installed in room A. Room B has been modified from a commercial low-constant-temperature room. To stabilize the temperature precisely around the environment of the interferometer, a low-temperature-stabilized cell is set on a passive antivibration table in room B. The cell is modified from the room-temperature-stabilized cell[3]. The cell is linked with a commercial-constant temperature refrigerant liquid bath (CTRLB), which is set in room C. In the cell, temperature-stabilized refrigerant liquid (ethyl alcohol) flows from the CTRLB to the cell. A measuring interferometer block, the supporting material of which is the ULTEG, is fixed inside the gas chamber. In the gas chamber, temperature and pressure sensors are set to determine or compensate the air-refractive-index using the Ciddor equation[4], when air is filled into the chamber. He gas with a pressure of around 102kPa can be filled as an alternative option to stabilize the refractive-index fluctuation[5]. Around the interferometer block, temporal and spatial temperature fluctuations are assumed to be less than 20mK for 40 days or more, because of the symmetry of the cell and heat isolation walls. The laser light is delivered from the frequency offset-lock laser in room A to the interferometer block at the gas chamber in room B through the PM fiber.

2.2 Interferometer

Figs. 2 (a) and (b) show the schematic diagram of the optical interferometer and its photograph. The operation of the interferometer is divided into two modes. One mode is a normal homodyne technique[6] and the other is a modified phase modulation homodyne technique[1,2]. The light source of the interferometer is the frequency offset-lock He-Ne laser. The frequency of the offset-lock He-Ne laser is compared with the frequency of an iodine-frequency-stabilized He-Ne laser and locked with the stability of 10^{-12} order. The light from the laser passes through the FR and is incident on the EOM. In the normal homodyne mode, the voltage applied to the EOM is null to keep the polarization state. In the phase modulation homodyne mode, in order to modulate the phase of the incident light and change its polarization, a sinusoidal modulation signal with a direct current (DC) offset is applied to the EOM. After the EOM and the HWP1, the light is incident on the PM fiber. The PM fiber is linked to the low-temperature-stabilized cell in room B. The main interferometer optics are mounted on a block made of the ULTEG (thermal expansion ratio=$2*10^{-8}K^{-1}$@-20˚C) to decrease optical path deformation in the interferometer owing to temperature change. In the phase modulation homodyne mode, to check the polarization state at the entrance of the interferometer, a small portion of the incident light is picked up by beam sampler (BS), polarization beam splitter 5 (PBS5) with a-45 polarization degree, and photodiode 5 (PD5). The rest of the light is then incident on polarization beam splitter 1 (PBS1) and divided into two arms of the interferometer. In Fig. 2 (a), the transmitted light from PBS1 passes through D-arm and A-arm and reaches to PBS2. In Fig. 2 (a), the reflected light from PBS1 goes through B-arm and C-arm and reaches to PBS2. In Fig. 2 (a), QWP, CC, NPBS and M are a quarter-wave plate, a corner cube, a nonpolarization beam splitter and a mirror, respectively. The CC3 and CC7 are set at the top of the ice deformation stage 1 and 2. To enhance the resolution of the interferometer, the 4-path configuration[2] is utilized between CC1, CC2, CC3, CC4, CC5, CC6, CC7 and CC8. As shown in Fig. 2 (b), two ice specimens were set at two parallel spring stages in the containers filled with the silicon oil to avoid sublimation or condensation on the ice surface. To maintain the stress direction against the ice, pitch, yaw and roll motions of the stage can be reduced to 0.5~5μrad for the maximum travel (~20μm). One stage has a weight load (100g-1kg) to induce strain against the ice specimen. The load of the other stage can be neglected. All optics except CC3 and CC7 are fixed on the ULTEM block with super invar and stainless-steel holders. The two beams of light from the two arms are recombined at PBS2. The recombined light passes through M5, HWP3, NPBS, PBS3&4 and QWP5, and then reaches to photodetector1-4 (PD1-4). To reduce the waste heat from PDs, only PD1, PD2 and PD5 are used in displacement measurement. In the normal homodyne mode, the output signals from PD1 and PD2 are utilized to make a Lissajous diagram for determining the optical path difference of the interferometer. In the modified phase modulation homodyne mode, the output signals from PD1, PD2 and PD5 are linked to the lock-in amplifiers (LIAs), and are demodulated with the modulation signal of the OSC, as shown in Fig. 3. The demodulated signals from LIA2 and 3 in Fig. 3 are used to make a Lissajous diagram for determining the optical path difference of the interferometer. The interferometer can measure the optical path difference of (Aarm+Darm)-(Carm+Barm), which is equivalent to (displacement difference between loaded (CC7) and unloaded (CC3) ice specimens)-(displacement difference between CC1 and CC5 at the basement of the block). To cancel the displacement due to thermal expansion (~$4*10^{-5}K^{-1}$@-20˚C) of ice specimen, displacement difference between loaded and unloaded ice, the manufacturing process and initial length of which must be the same, is measured.

The light intensities I_{PD1} and I_{PD2} at PD1 and PD2 are

$$I_{PD1} = \frac{1}{2}\left\{E_x^{\,2} + E_y^{\,2} - 2E_xE_y\cos(\delta_E + \delta_P + \delta_I)\right\} \quad (1),$$

$$I_{PD2} = \frac{1}{2}\left\{E_x^{\,2} + E_y^{\,2} - 2E_xE_y\cos(\delta_E + \delta_P + \delta_I - \frac{\pi}{2})\right\} \quad (2),$$

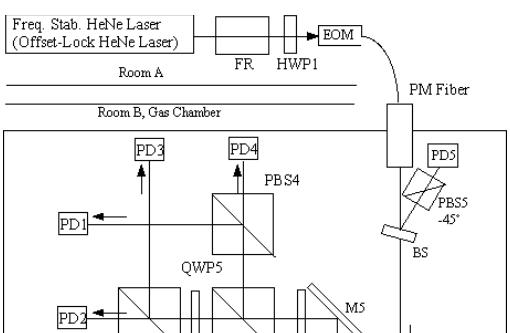

Fig. 2 (a) Optical interferometer system and (b) photograph of optical interferometer. PD: photodiode, PBS: Polarization beam splitter, NPBS nonpolarizing beam splitter, HWP: Half-wave plate, QWP: Quarter-wave plate, CC: Corner cube, BS: Beam sampler, M: Mirror, FR: Faraday rotator. The two ice specimens and two deformation stages were set in the containers filled with the silicon oil.

where, E_x, E_y, δ_E, δ_P and δ_I are electric field amplitude of the incident light, the retardations for the EOM/PM fiber and the phase shift due to the optical path difference in the interferometer. In the normal homodyne mode, we assume that no retardations originate from the EOM and the PM fiber (δ_E=δ_P=0). Therefore, we obtain

$$I_{PD1} = \frac{1}{2}\left\{E_x{}^2 + E_y{}^2 - 2E_xE_y\cos(\delta_I)\right\} \quad (3),$$

$$I_{PD2} = \frac{1}{2}\left\{E_x{}^2 + E_y{}^2 - 2E_xE_y\cos(\delta_I - \frac{\pi}{2})\right\} \quad (4).$$

From equations (3) and (4), δ_I can be determined using the Lissajous diagram. δ_I is written as

$$\delta_I = 16\pi\frac{x}{\lambda} \quad (5),$$

where x and λ are the change in the optical path difference (~ displacement of the ice specimen) of the interferometer and the wavelength of the laser, respectively.

Under real operational conditions, the retardation fluctuation from the PM fiber cannot be neglected, because the fiber is affected by disturbances (vibration and thermal variation). To overcome retardation fluctuation, we use the phase modulation homodyne interferometer technique. In the technique, the retardation of δ_E consists of two components as follows:

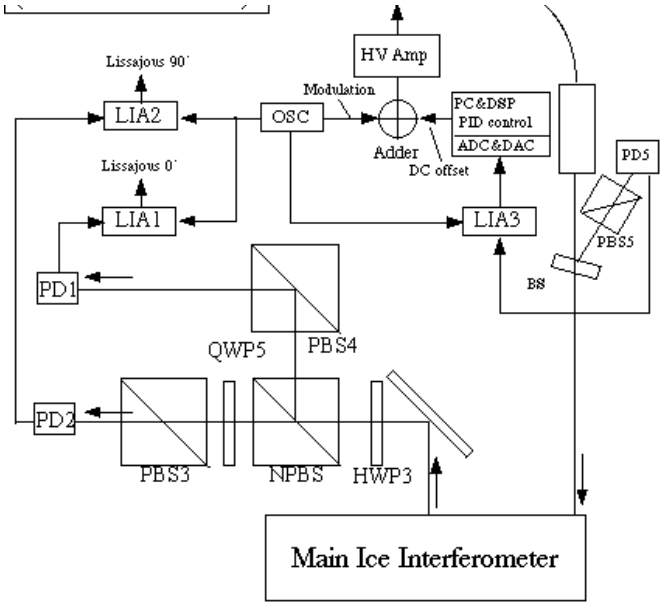

Fig. 3 Control system for modified phase modulation homodyne interferometer. LIA: Lock-in amplifier, PID: Proportional-integral-derivative, HV Amp: High voltage amplifier.

$$\delta_E = \delta_{EDC} + m\cos\omega t \quad (6),$$

where δ_{EDC}, m and ω are the DC offset retardation, modulation depth and angular modulation frequency, respectively. LIA signal I_{LIA3} for I_{PD5} is written as[1]

$$I_{LIA3} = -\frac{1}{2}E_xE_y\sin(\delta_{EDC} + \delta_P)\times J_1(m) \quad (7),$$

where $J_1(m)$ is the 1st-order Bessel function. At the null point of the lock-in signal I_{LIA3}, $\delta_{EDC} + \delta_P = 0$. This means that the fluctuation of δ_P can be compensated by adjusting or controlling δ_{EDC} by the null method. In Fig. 3 the lock-in signal I_{LIA3} is locked to be null by the PC

& DSP (PID) controller. From equations (1), (2) and (7) under the condition of $\delta_{EDC} + \delta_P = 0$, the LIA signals I_{LIA1} and I_{LIA2} for I_{PD1} and I_{PD2} can be represented by

$$I_{LIA1} = -\frac{1}{2} E_x E_y \sin(\delta_I) \times J_1(m) \quad (8),$$

$$I_{LIA2} = -\frac{1}{2} E_x E_y \sin(\delta_I - \frac{\pi}{2}) \times J_1(m) \quad (9).$$

Therefore, δ_I can also be determined using the Lissajous diagram from the two LIA signals shown in equations (8) and (9). The ice strain rate $S(t)$ at the time of t can be expressed as,

$$S(t) = \frac{x(t+\Delta T) - x(t)}{L\Delta T} = \frac{\lambda\{\delta_I(t+\Delta T) - \delta_I(t)\}}{16\pi L\Delta T} \quad (10).$$

In equation (10), $x(t)$, L, ΔT and $\delta_I(t)$ are the displacement of the ice specimen at the time of t, the initial length of the ice specimen, the standard sampling time and the measured phase at the time of t, respectively.

3. Ice strain rate measurement

In order to test the feasibility of the proposed measurement system, the strain rate of artificial polycrystalline ice was measured[7]. The manufacturing process of the ice specimens (loaded and unloaded ice specimens) and the experimental conditions are listed at Table 1. Figs. 4 (a) and (b) show time variations of the displacement of the loaded ice specimen and the temperature/pressure of air environment in the gas chamber, respectively. As shown in Fig. 4 (b), maximum temperature instability was 5mK for 14 hours. In the experiments, the shield condition of the chamber was not perfect. Fig. 5 shows the time variation of the strain rate of the ice specimen for 45days using the equation (10). In the strain rate calculation, we assumed that L and ΔT are 58.5mm and 10minutes (600s), respectively.

The displacement change in the selected period in Fig. 5 (around 8th day) is shown in Fig. 4 (a). In Fig. 4 (a), the first and last halves indicate the results obtained using the normal and modified phase modulation modes. The air-refractive-index fluctuation arising from temperature and pressure changes shown in Fig. 4 (b) was calculated and compensated to determine λ in equations (5) and (10) using the Ciddor equation[4]. Fig. 4 (a) shows the compensated result. Fig. 5 shows that strain rate of $10^{-10}s^{-1}$ or less can be measured using our proposed system.

The total estimated uncertainty (k=1) for normal and modulation homodyne modes were $1.5*10^{-10}s^{-1}$ and $8.1*10^{-11}s^{-1}$, respectively. The uncertainty sources are A) phase measurement, B) air refractive index compensation, C) laser frequency fluctuation, D) Abbe error, E) cosine error, F) the length difference between the loaded and unloaded ice specimens and so on.

Table 1 Processing and experimental conditions for the present ice creep tests.

	Loaded ice	Unloaded ice
Initial length mm	58.55	57.55
Diameter mm]	19.82	19.45
Density kg/m^3	919.5	928.4
Grain size mm	8~12	8~12
Stress MPa	0.016	------
Temperature	-25˚C	-25˚C

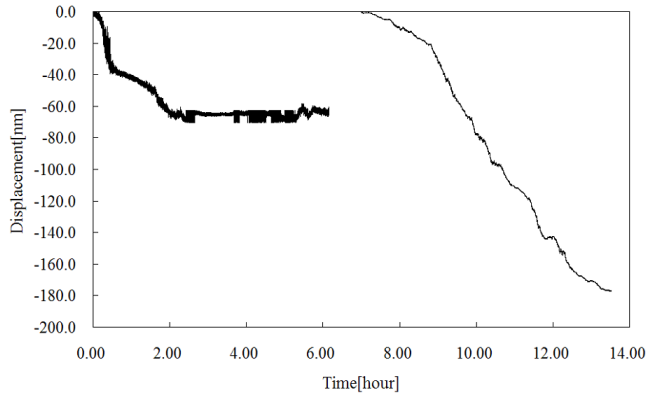

(a)

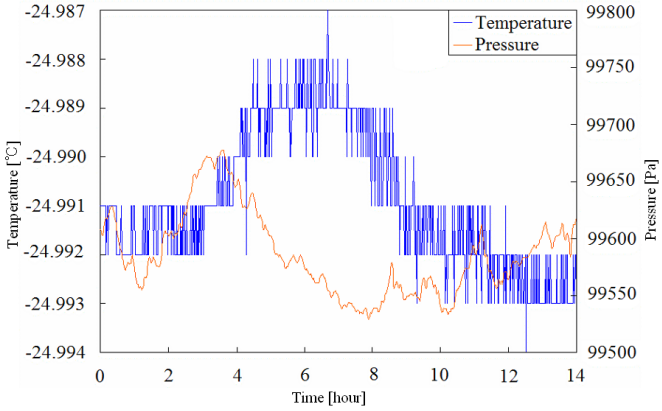

(b)

Fig. 4 (a) Time variation of displacement of ice and (b) time variation of temperature and pressure of air in gas chamber.

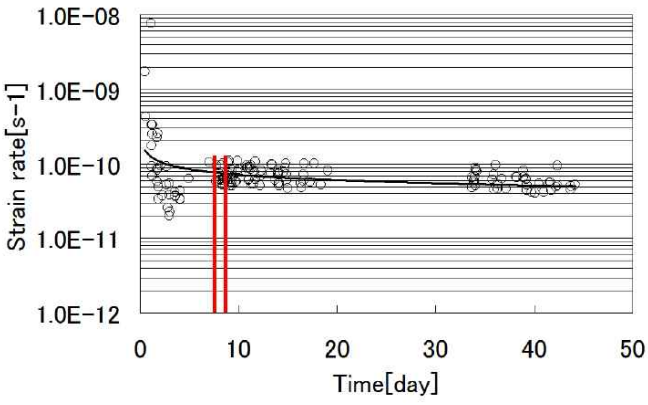

Fig. 5 Time variation of the strain rate of the ice specimen for 45days.

4. Conclusions

The analysis of the flow behavior of the Antarctic ice sheet ice provides information on past climate changes of Earth. To understand the ice flow behavior, ice creep strain rate measurement is important. In this study, an ice creep strain rate measurement system with an uncertainty of $8.1*10^{-11}s^{-1}$ was developed. The modified phase modulation homodyne interferometer, the supporting material of which is ultralow-thermal-expansion glass, was combined with the system to measure the ice deformation. In the system, the typical displacement resolution and measurement time (or sampling time) are of nanometer scale or less and 10minutes, respectively. To maintain

the experimental conditions for ice creep, the low-temperature-stabilized cell with temperature stability of 5mK for 10hours and 20mK for 45days and an ice deformation stage with a parallel spring structure as a guide were developed. With the use of this system, the ice strain rate of less than $10^{-10}s^{-1}$, which is comparable to the estimated measurement uncertainty of $8.1*10^{-11}s^{-1}$, can be measured for a short period of 10minutes.

ACKNOWLEDGEMENT

Financial support from the Scientific Research Fund of the Japanese Society for the Promotion of Science (JSPS) is gratefully acknowledged.

REFERENCES

1. Basile G., Bergamin A., Cavagnero G. and Mana G., "Phase modulation in high-resolution optical interferometry," Metrologia, Vol. 28, pp. 455-461, 1991.
2. Ishige M., Matsuura F., Kawasugi M. and Aketagawa M. "Phase-modulation-homodyne interferometer with 10 picometer resolution using tunable laser diode," International Journal of Precision Engineering and Manufacturing, Vol. 8 pp. 80-84, 2007.
3. Aketagawa M., Takada K., Kobayashi K., Takeshima N., Noro M. and Nakayama Y. "Length measurement using regular crystalline lattice and a dual tunneling unit scanning tunneling microscope in a thermo-stabilized cell," Mea. Sci. Technol. Vol. 9, pp. 1076-1081, 1998.
4. Ciddor P. E., "Refractive index of air: new equations for the visible and near infrared," Appl. Opt., Vol. 35, pp. 1566-1573, 1996.
5. Bryan J. B., "Design and construction of an ultraprecision 84 inch diamond turning machine," Precision Engineering, Vol. 1**,** pp. 13-17, 1979.
6. Keem T., Gonda S., Misumi I., Huang Q. and Kurosawa T., "Removing nonlinearity of a homodyne interferometer by adjusting the gains of its quadrature detector system," Appl. Opt., Vol. 43, pp. 2443-2448, 2004
7. Aketagawa M., Azuma N., Takata M., Sugawara R., Ito R., Anno K., Kogure T., Ohba Y., "Ultraslow strain rate measurement system for ice using a modified phase modulation homodyne interferometer," Mea. Sci. Technol., Vol. 22, 035702, 2011.